Supplementary Information

Isolation, Absolute Configuration and Cytotoxic Activities of Alkaloids from *Hippeastrum goianum* (Ravenna) Meerow (Amaryllidaceae)

Mariacaterina Lianza, [#,a,b] ***Maria Helena Verdan,*** [#,b] ***Jean Paulo de Andrade,*** [b,c] ***Ferruccio Poli,*** [a] ***Larissa C. de Almeida,*** [d] ***Leticia V. Costa-Lotufo,*** [d] ***Álvaro Cunha Neto,*** [b] ***Sarah C. C. Oliveira,*** [e] ***Jaume Bastida,*** [f] ***Andrea N. L. Batista,*** [g] ***João M. Batista Jr.*** [h] ***and Warley S. Borges*** *[,b]

[a]*Department of Pharmacy and Biotechnology, Almer Mater Studiorum, University of Bologna, CP 40126, Bologna, Italy*

[b]*Departamento de Química, Universidade Federal do Espírito Santo, 29075-910 Vitória-ES, Brazil*

[c]*Laboratorio de Química de Productos Naturales, Instituto de Química de Recursos Naturales, y Núcleo Científico Multidisciplinario, Dirección de Investigación, Universidad de Talca, CP 3460000, Talca, Chile*

[d]*Departamento de Farmacologia, Universidade de São Paulo, 05508-900 São Paulo-SP, Brazil*

[e]*Departamento de Botânica, Universidade de Brasília, 70910-900 Brasília-DF, Brazil*

[f]*Departament de Biologia, Sanitat i Medi Ambient, Facultat de Farmàcia i Ciències de l´Alimentació, Universitat de Barcelona, CP 08028, Barcelona, Spain*

[g]*Instituto de Química, Universidade Federal Fluminense, 24020-141 Niterói-RJ, Brazil*

[h]*Instituto de Ciência e Tecnologia, Universidade Federal de São Paulo, 12231-280 São José dos Campos-SP, Brazil*

*e-mail: warley.borges@ufes.br

[#]These authors contributed equally to this study.

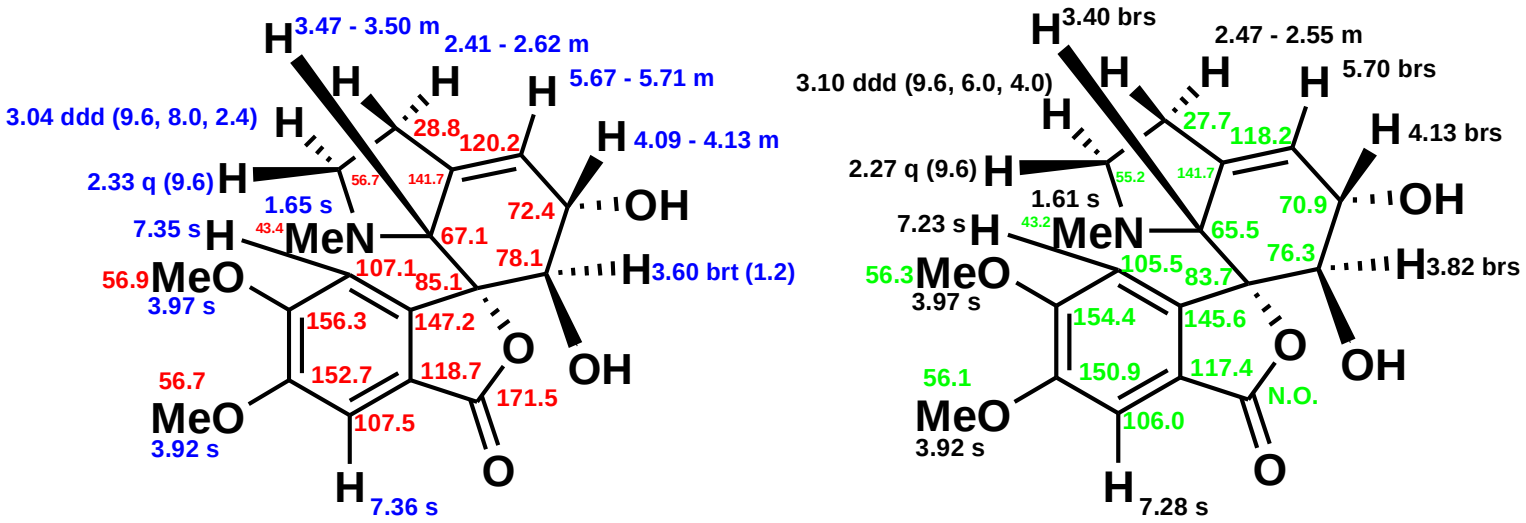

Figure S1. ^{1}H (blue) and ^{13}C (red) (400 MHz, MeOD) and ^{1}H (black) and ^{13}C (green) (400 MHz, $CDCl_3$) NMR chemical shifts (ppm) observed in the NMR data of the compound **1** (*J* in Hz).

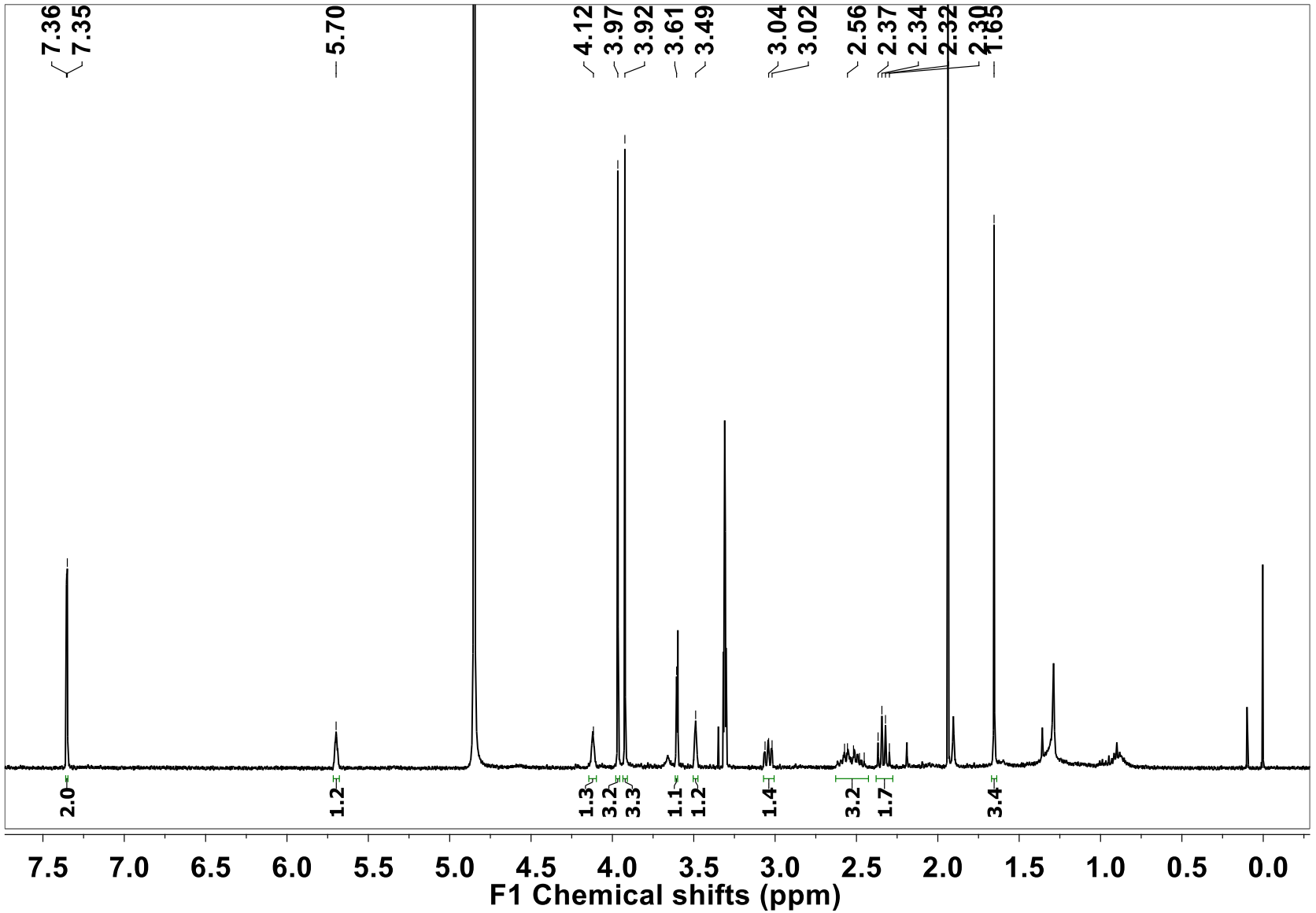

Figure S2. ^{1}H NMR spectrum of compound **1** (400 MHz, MeOD).

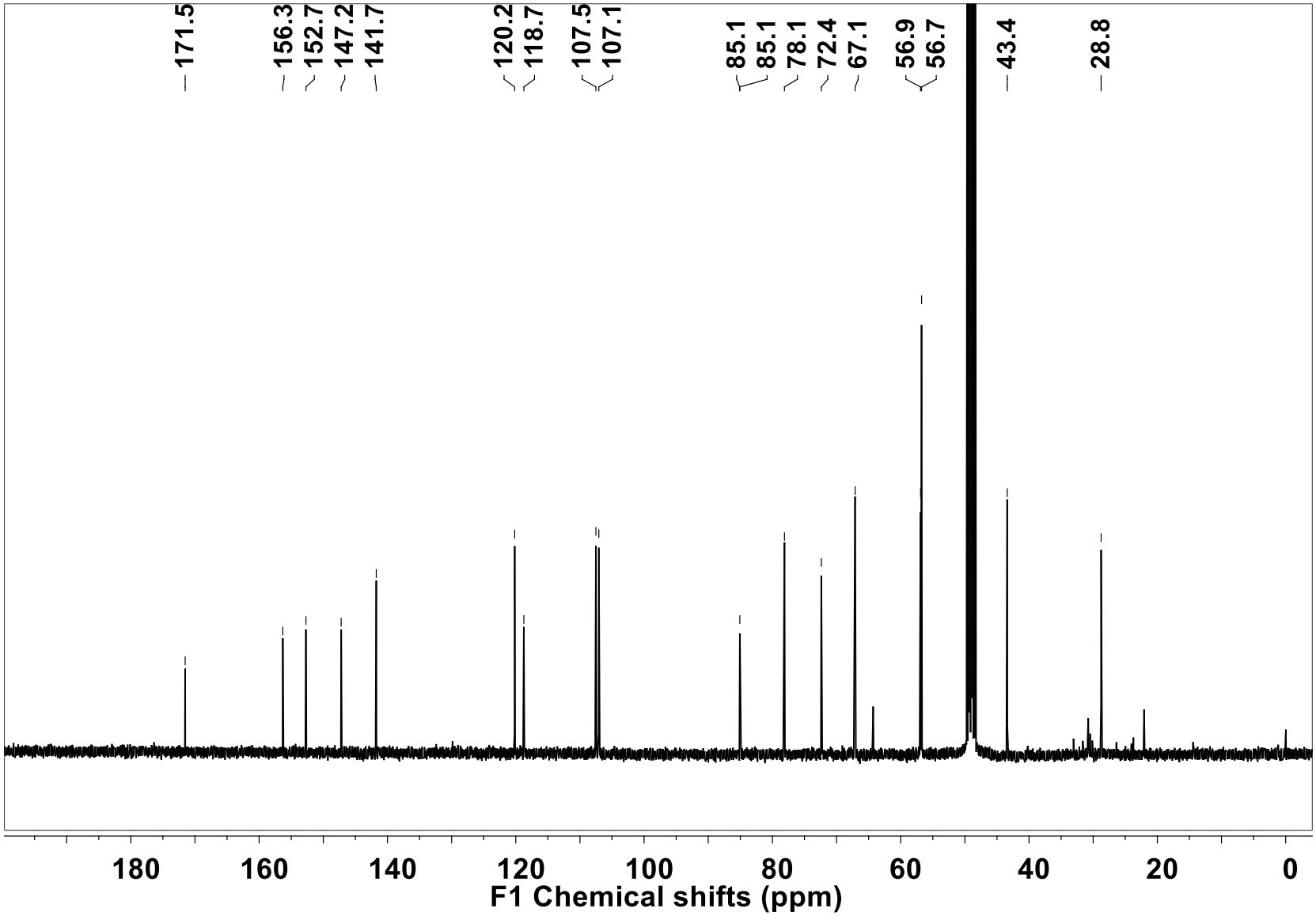

Figure S3. ^{13}C NMR spectrum of compound **1** (100 MHz, MeOD).

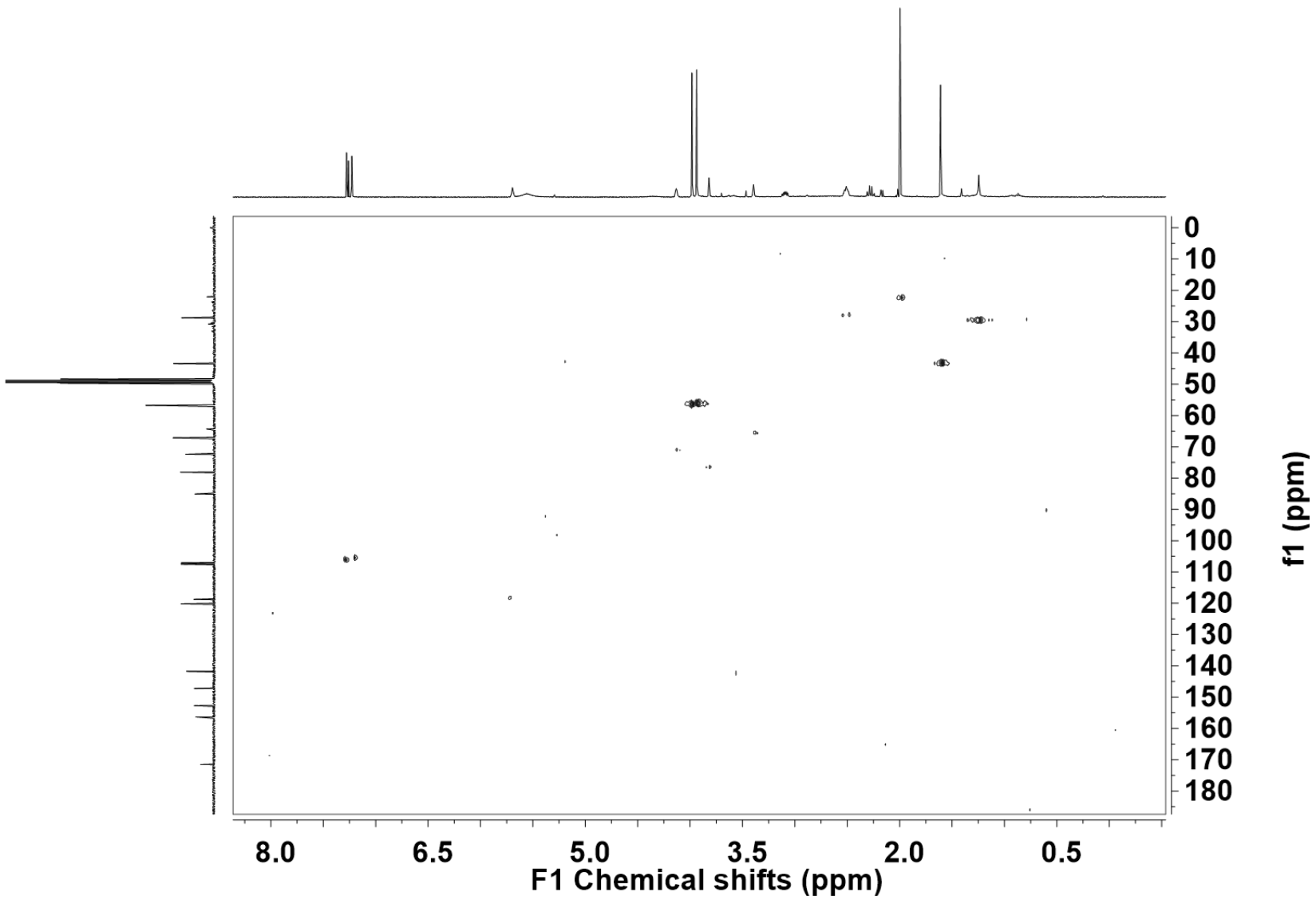

Figure S4. HSQC spectrum of compound **1** (400 MHz, MeOD).

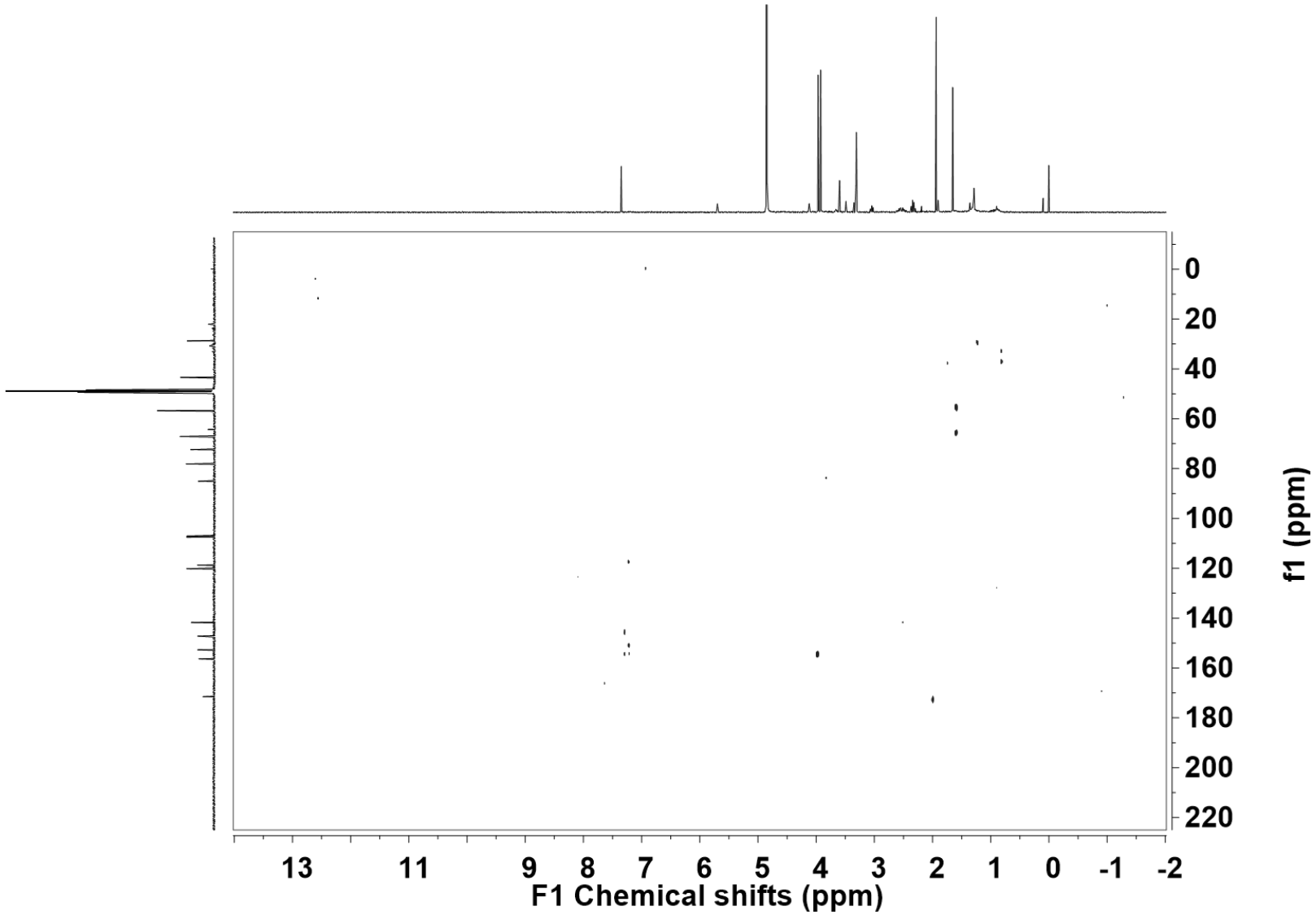

Figure S5. HMBC spectrum of compound **1** (400 MHz, MeOD).

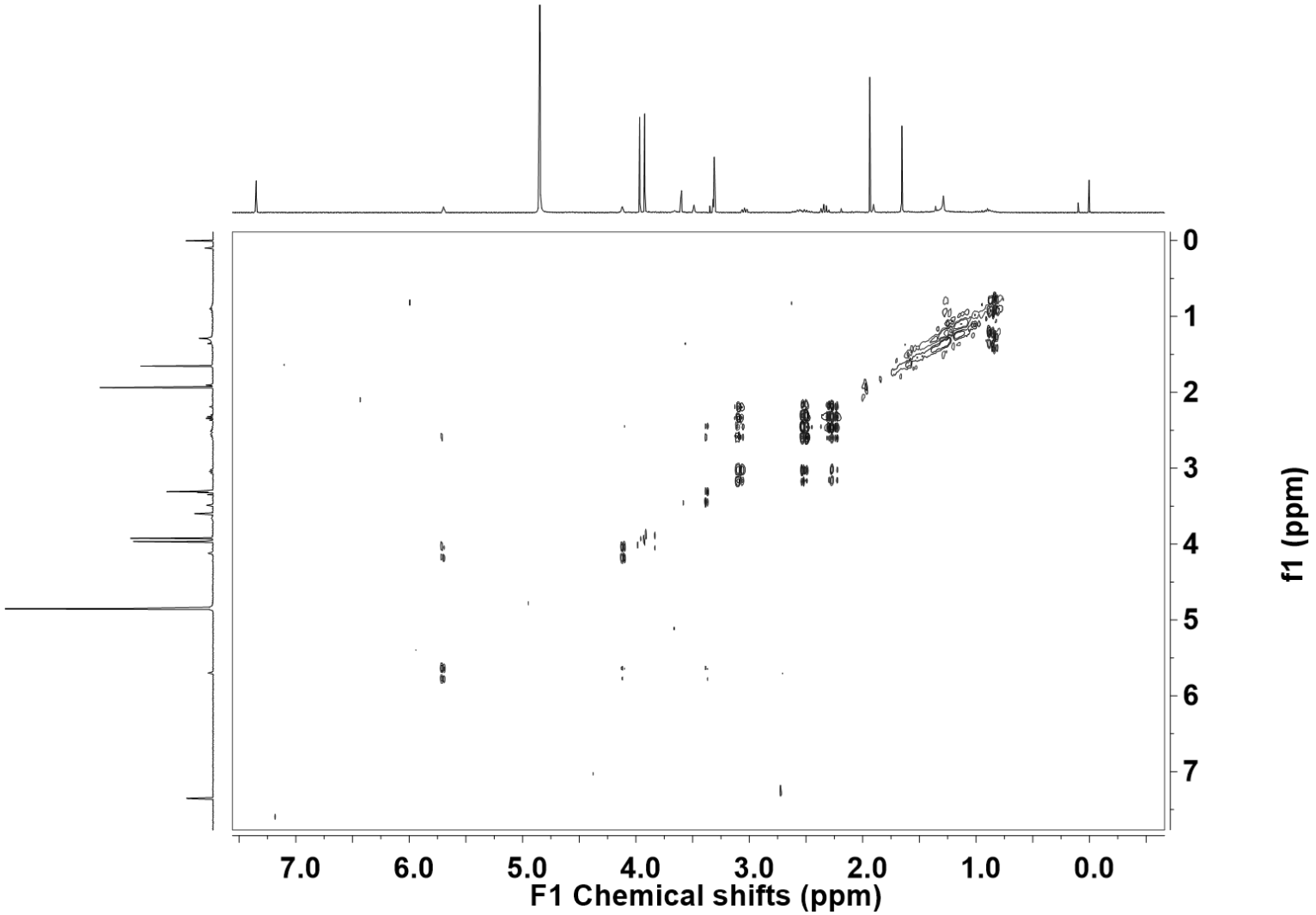

Figure S6. COSY spectrum of compound **1** (400 MHz, MeOD).

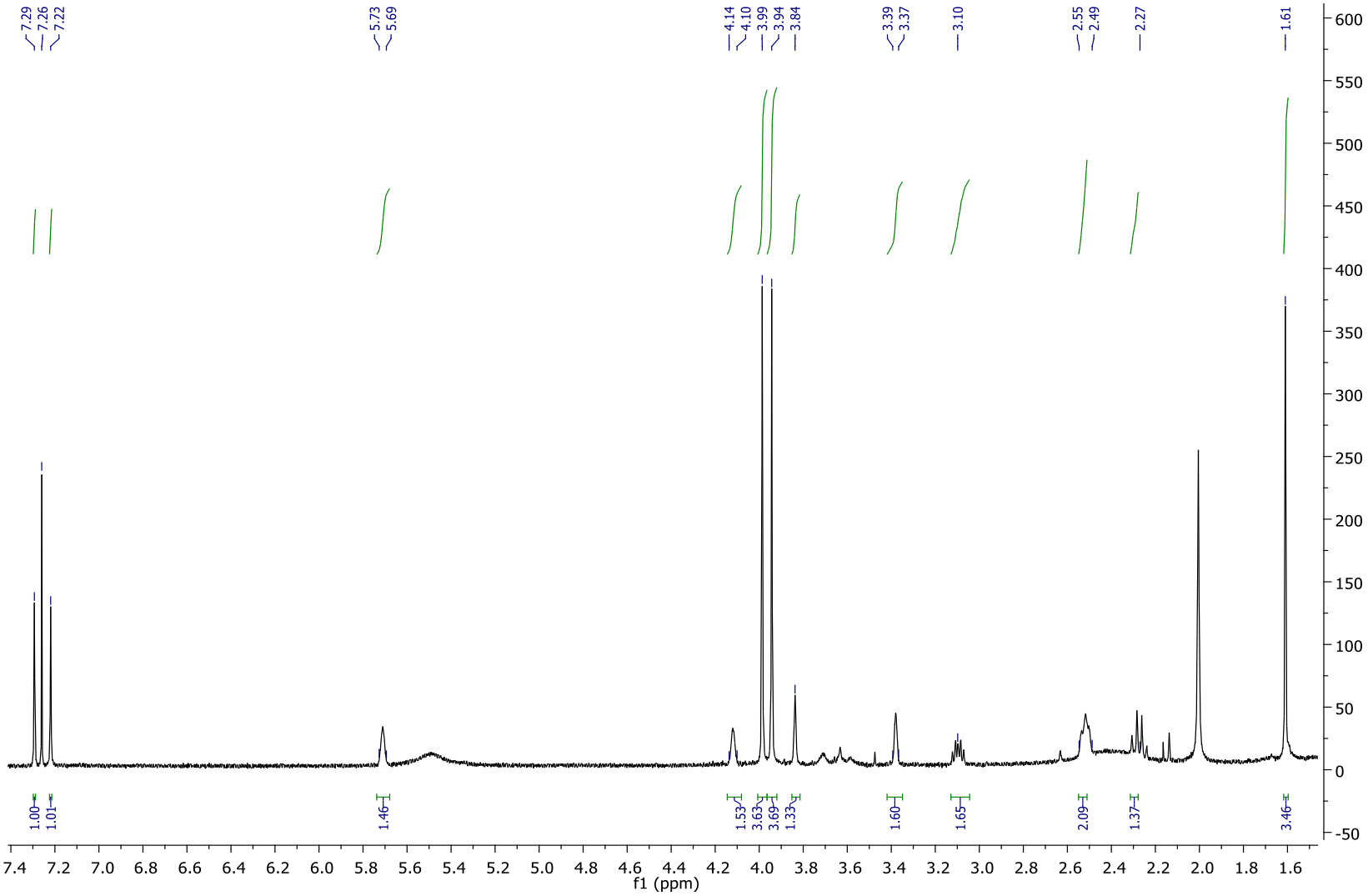

Figure S7. ^{1}H NMR spectrum of compound **1** (400 MHz, $CDCl_3$).

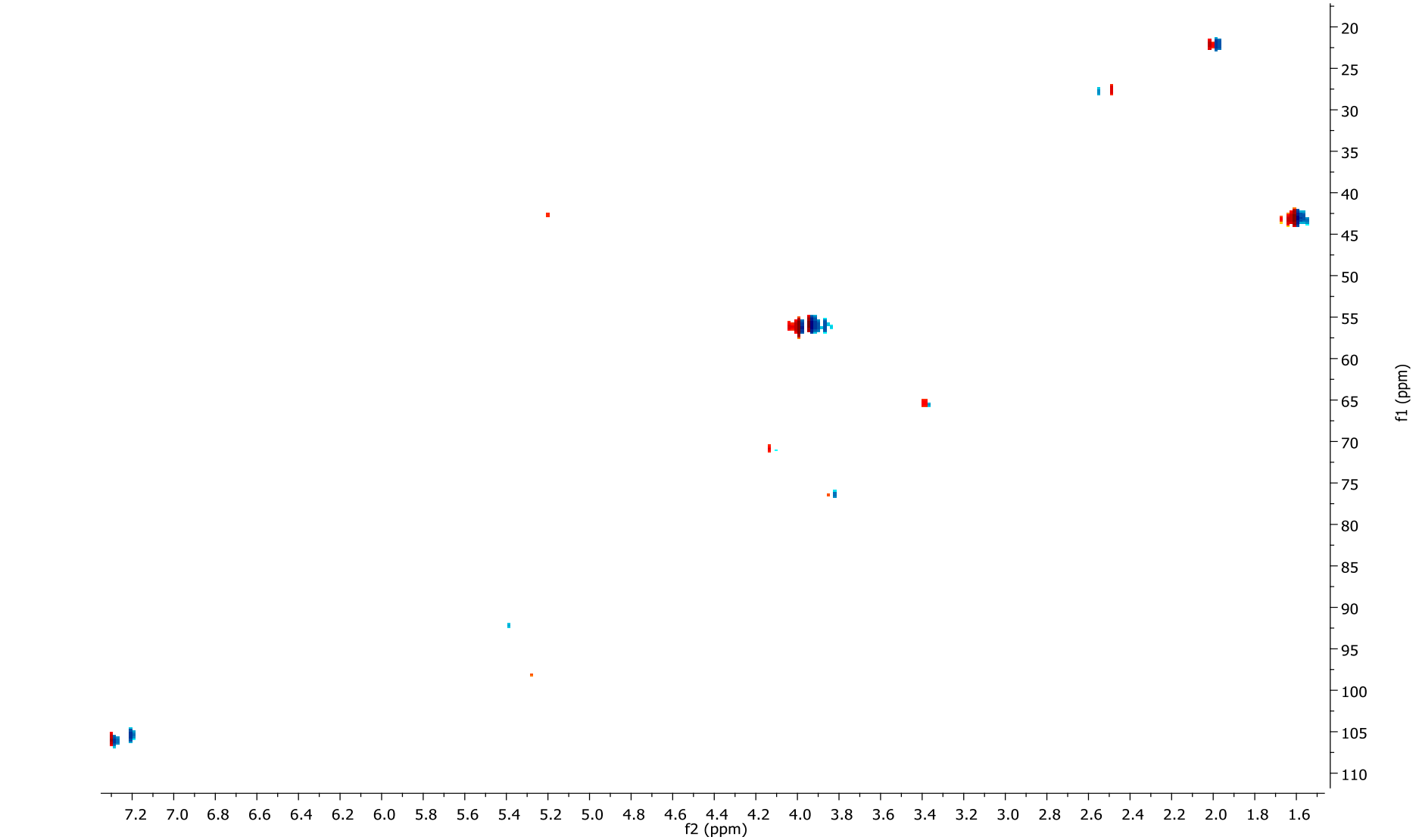

Figure S8. HSQC spectrum of compound **1** (400 MHz, $CDCl_3$).

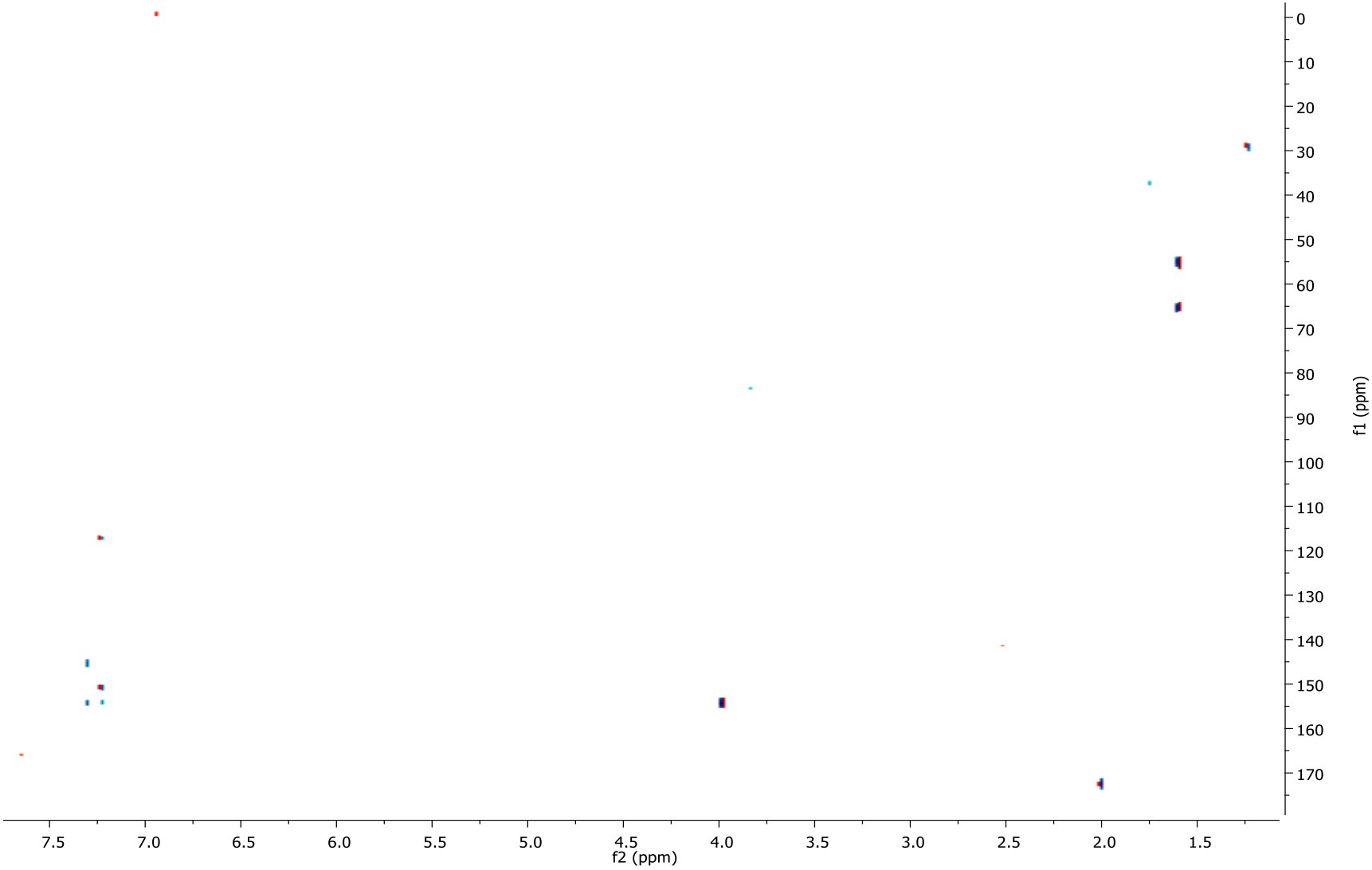

Figure S9. HMBC spectrum of compound **1** (400 MHz, $CDCl_3$).

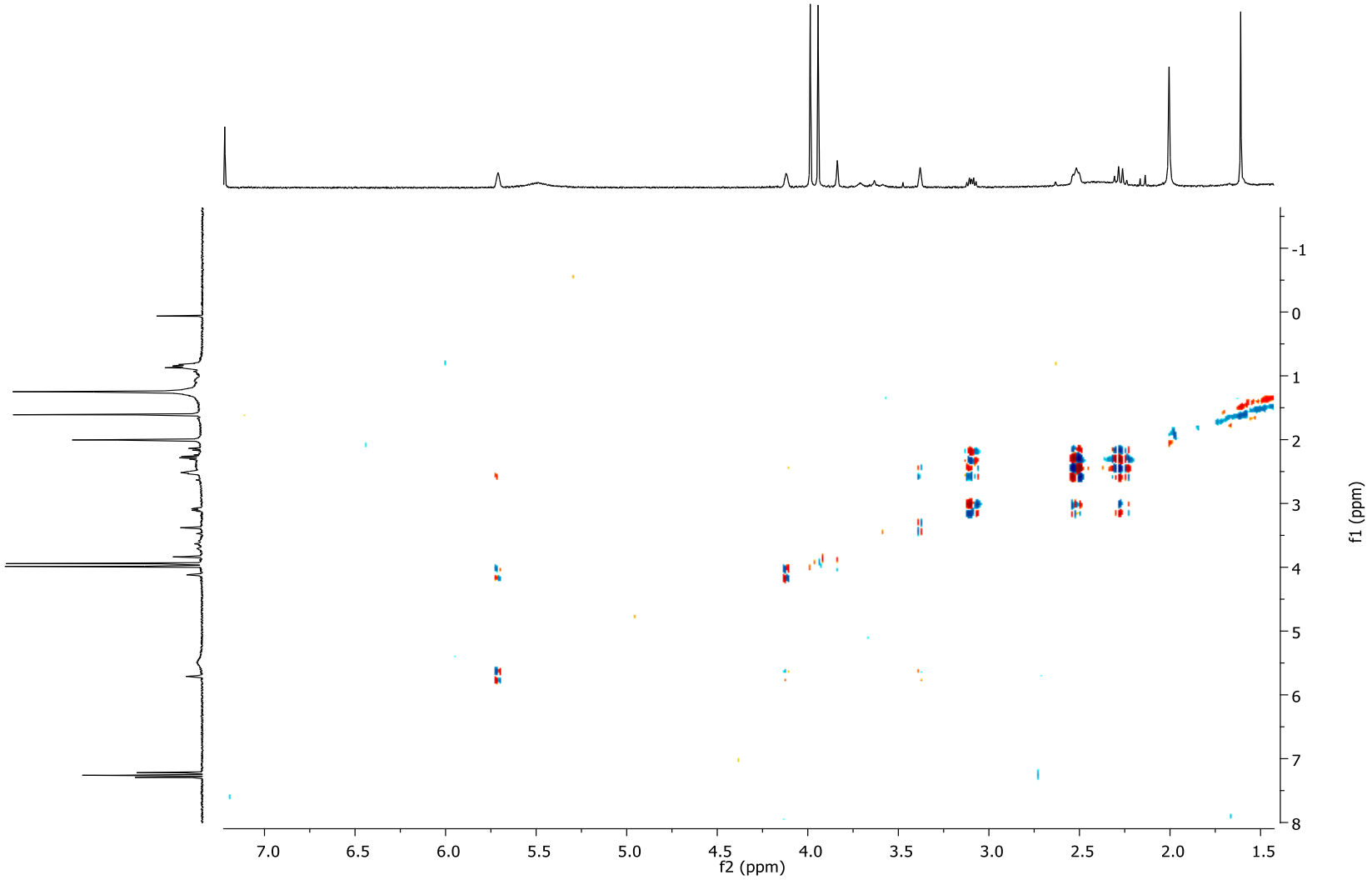

Figure S10. COSY spectrum of compound **1** (400 MHz, $CDCl_3$).

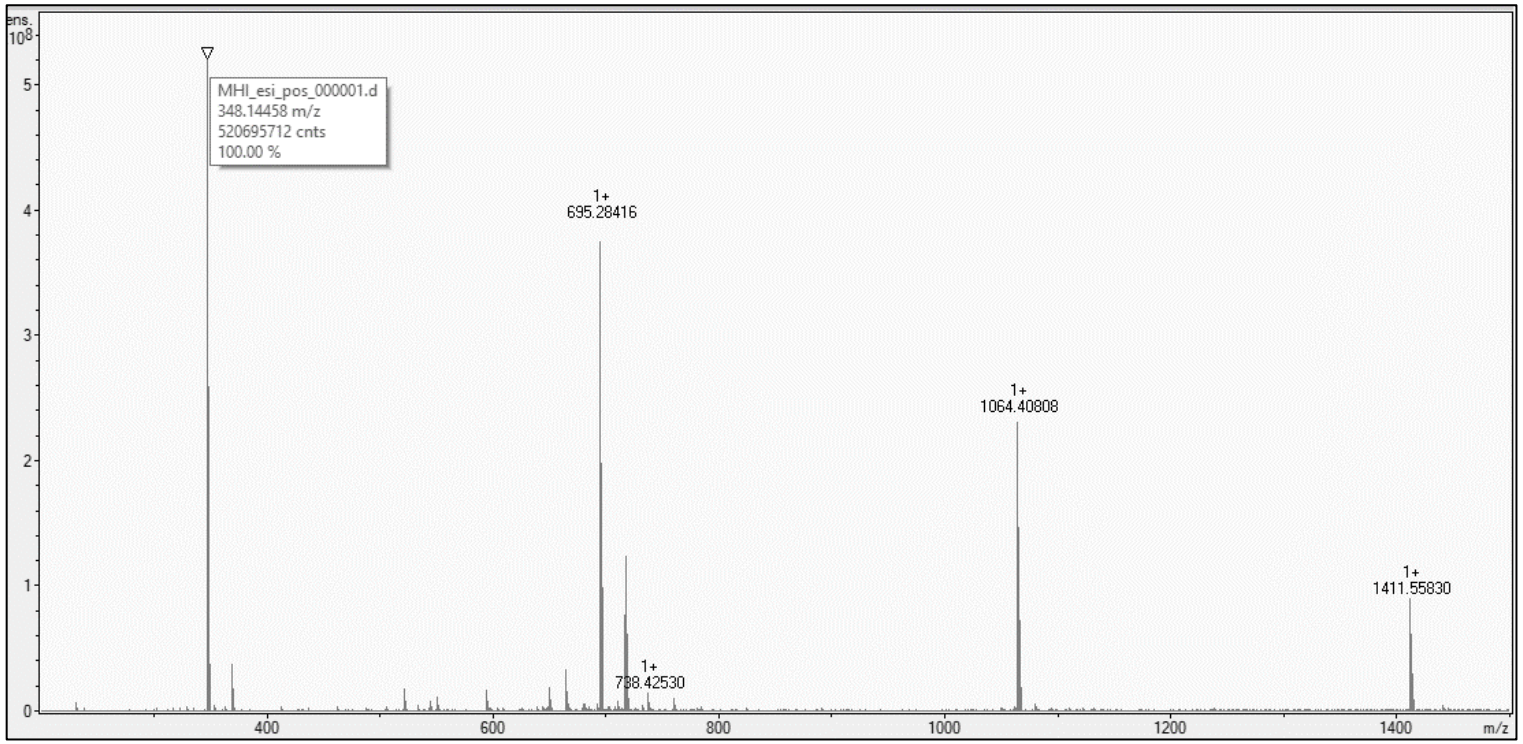

Figure S11. HRESIMS spectrum of compound **1**.

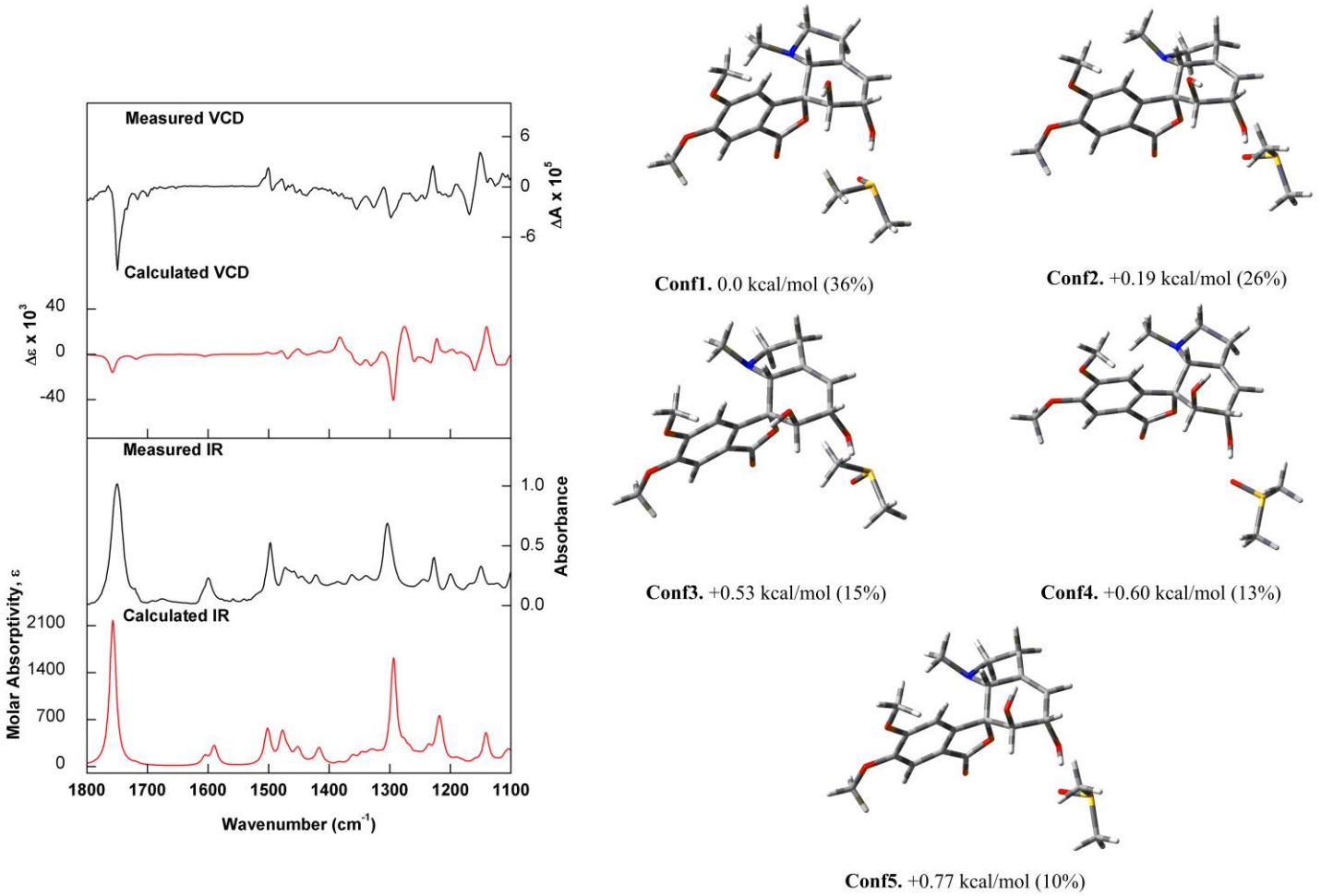

Figure S12. (Left) Comparison of the observed IR and VCD spectra of compound **1** in DMSO-d_6 with the calculated [B3LYP/PCM(DMSO)/6-31G(d)] IR and VCD spectra of the Boltzmann average of the lowest-energy conformers identified for (1*R*,2*S*,4a*R*,10b*R*)-**1**. (Right) Optimized structures including explicit solvent, relative Gibbs free energies, and Boltzmann population (%) of the lowest-energy conformers of (1*R*,2*S*,4a*R*,10b*R*)-**1** at the B3LYP/PCM(DMSO)/6-31G(d) level.

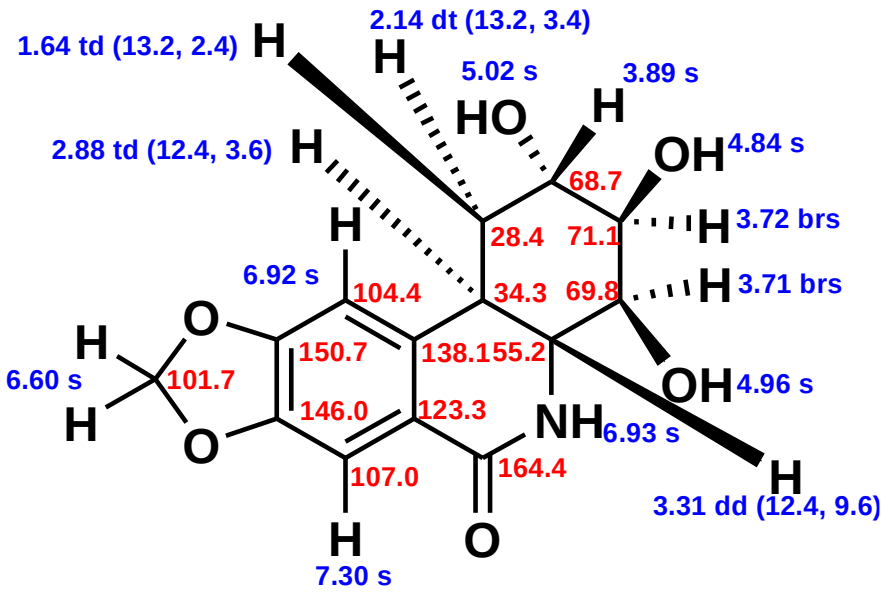

Figure S13. ^{1}H (blue, 400 MHz, DMSO-d_6) and ^{13}C (red, 100 MHz, DMSO-d_6) NMR chemical shifts (ppm) observed in the NMR data of the compound **2** (*J* in Hz).

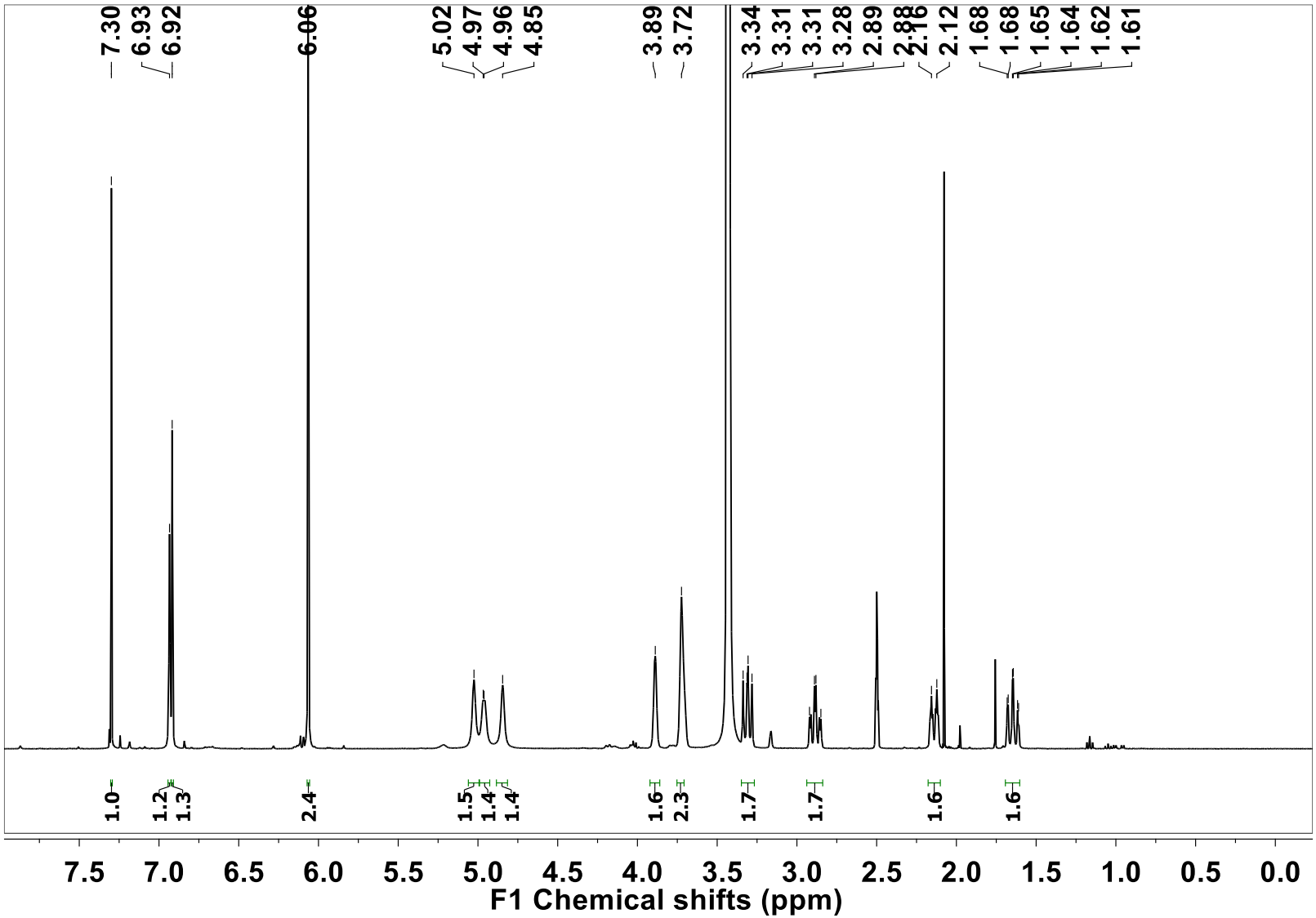

Figure S14. ^{1}H NMR spectrum of compound **2** (400 MHz, DMSO-d_6).

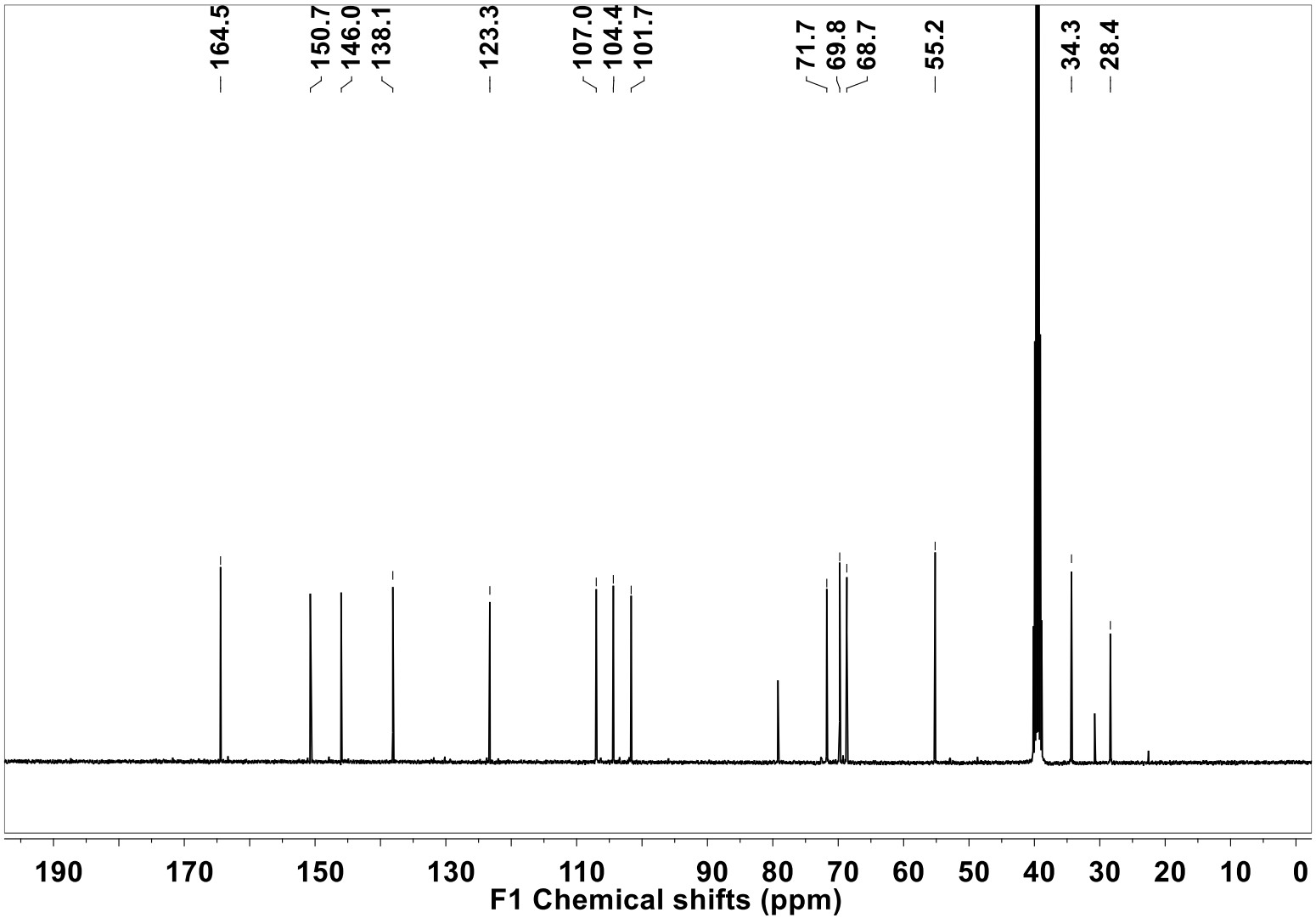

Figure S15. ^{13}C NMR spectrum of compound **2** (100 MHz, DMSO-d_6).

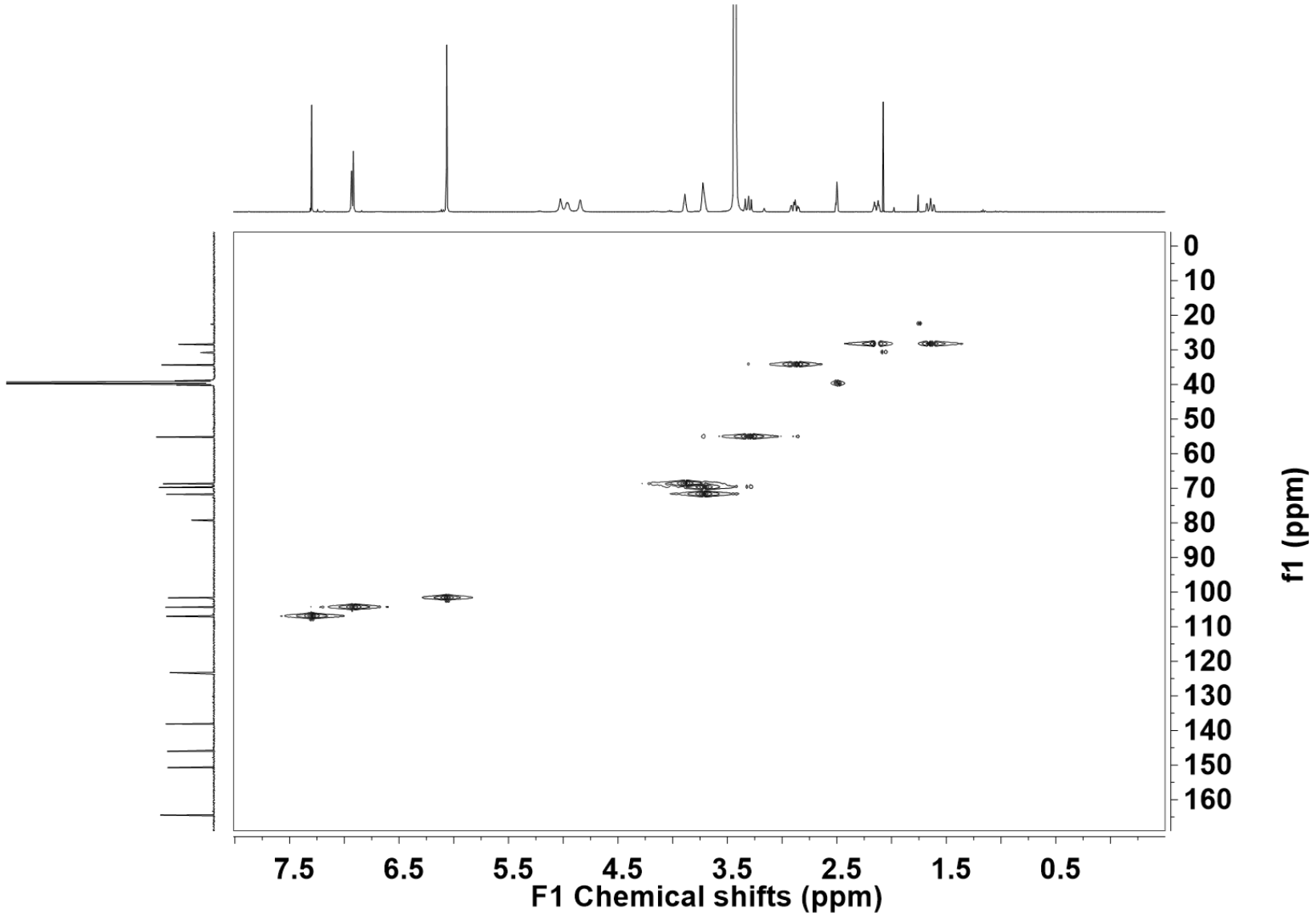

Figure S16. HSQC spectrum of compound **2** (400 MHz, DMSO-d_6).

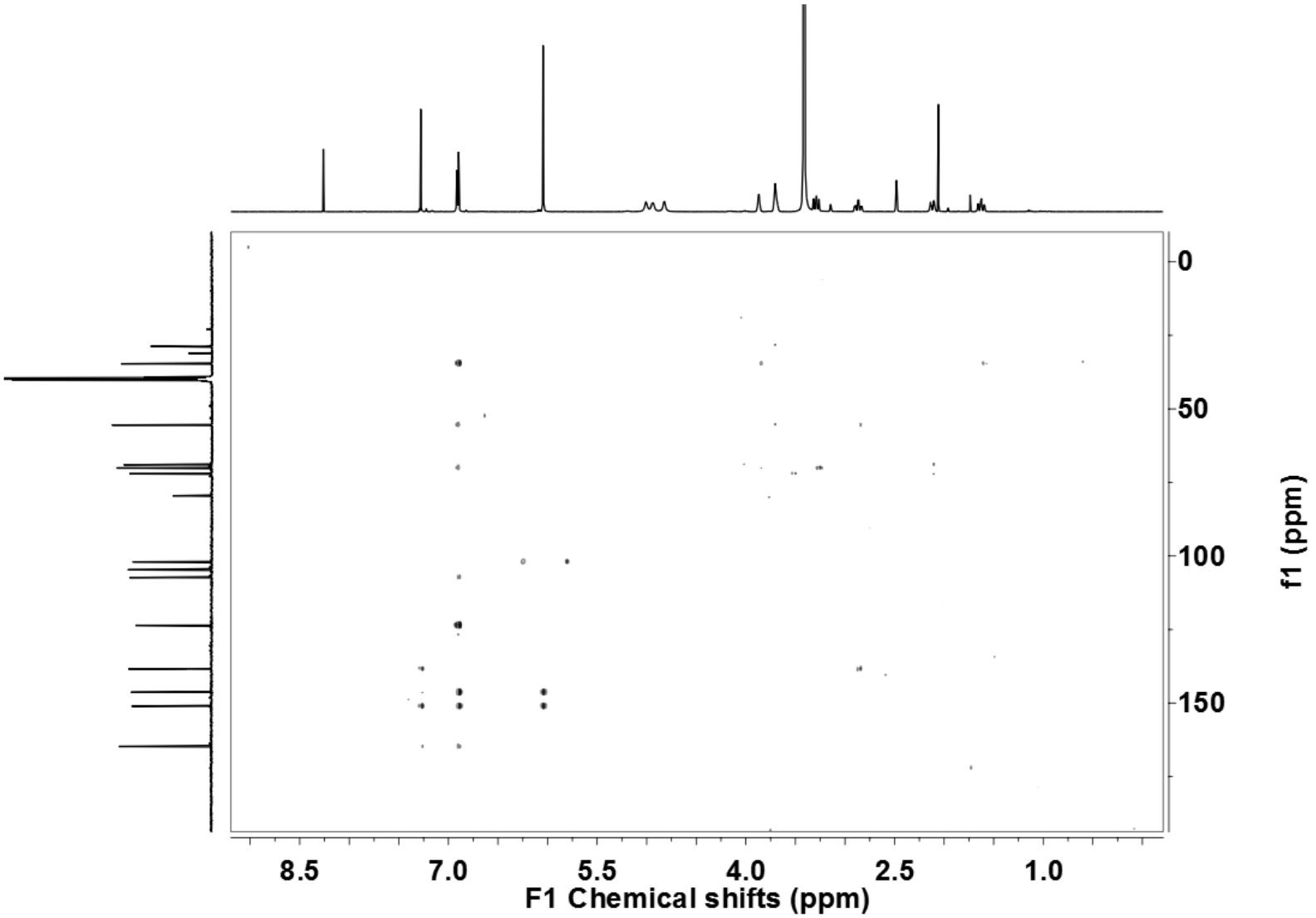

Figure S17. HMBC spectrum of compound **2** (400 MHz, DMSO-d_6)

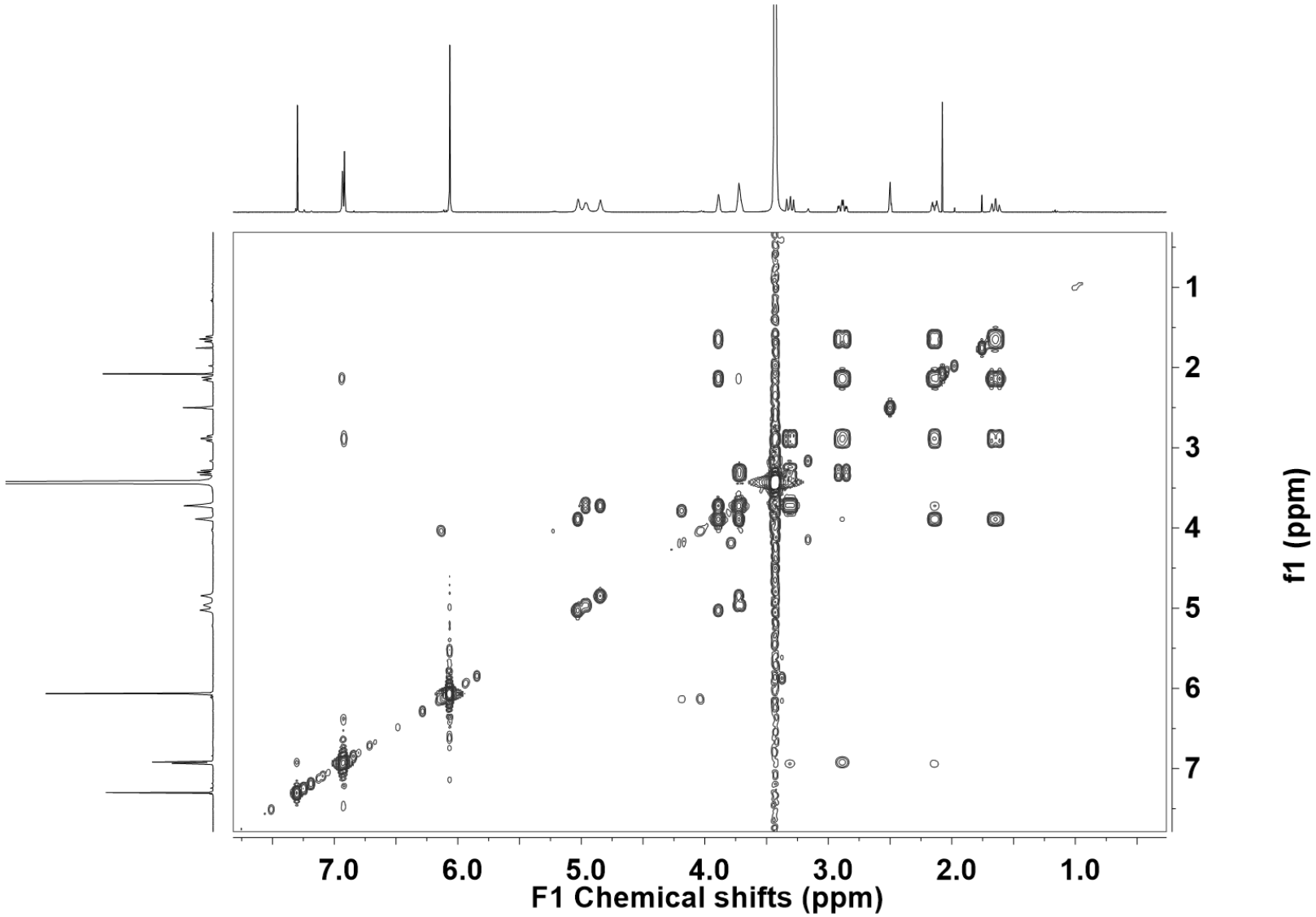

Figure S18. COSY spectrum of compound **2** (400 MHz, DMSO-d_6).

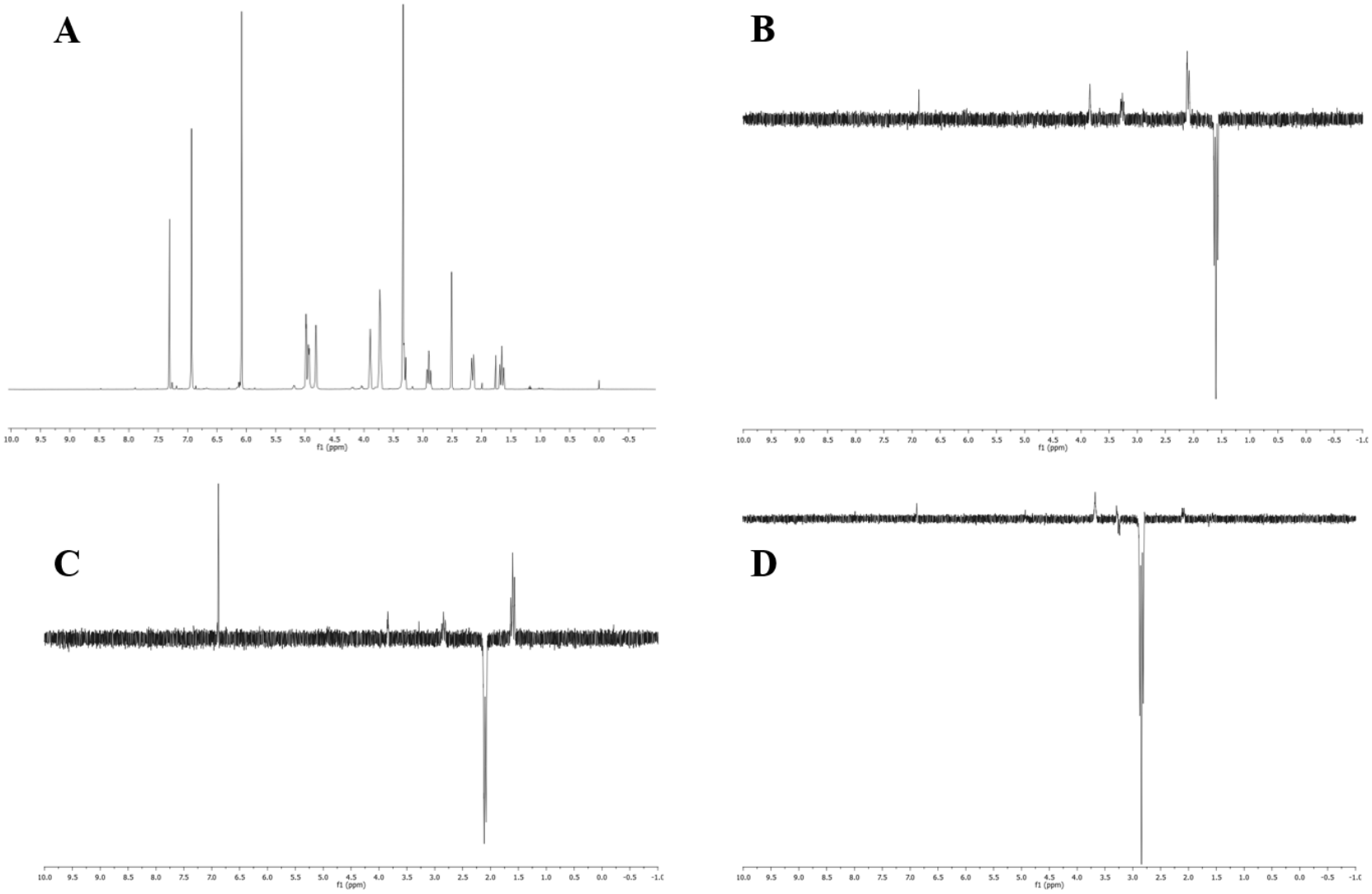

Figure S19. (a) ^{1}H NMR and NOE spectra of the compound **2** irradiated at: (b) 1.64 ppm, (c) 2.14 ppm and (d) 2.88 ppm. (400 MHz, DMSO-d_6).

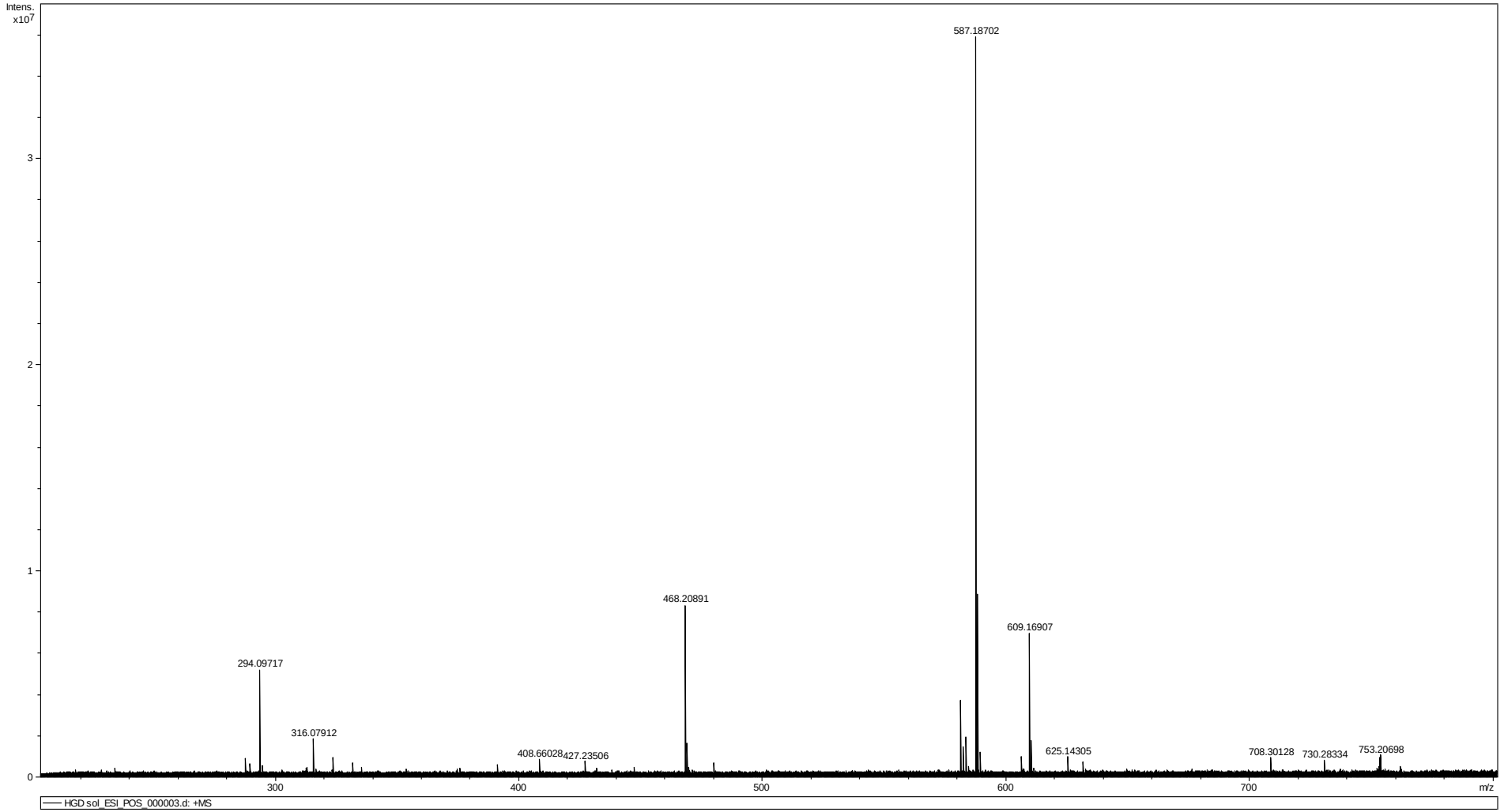

Figure S20. HRESIMS spectrum of compound **2**.

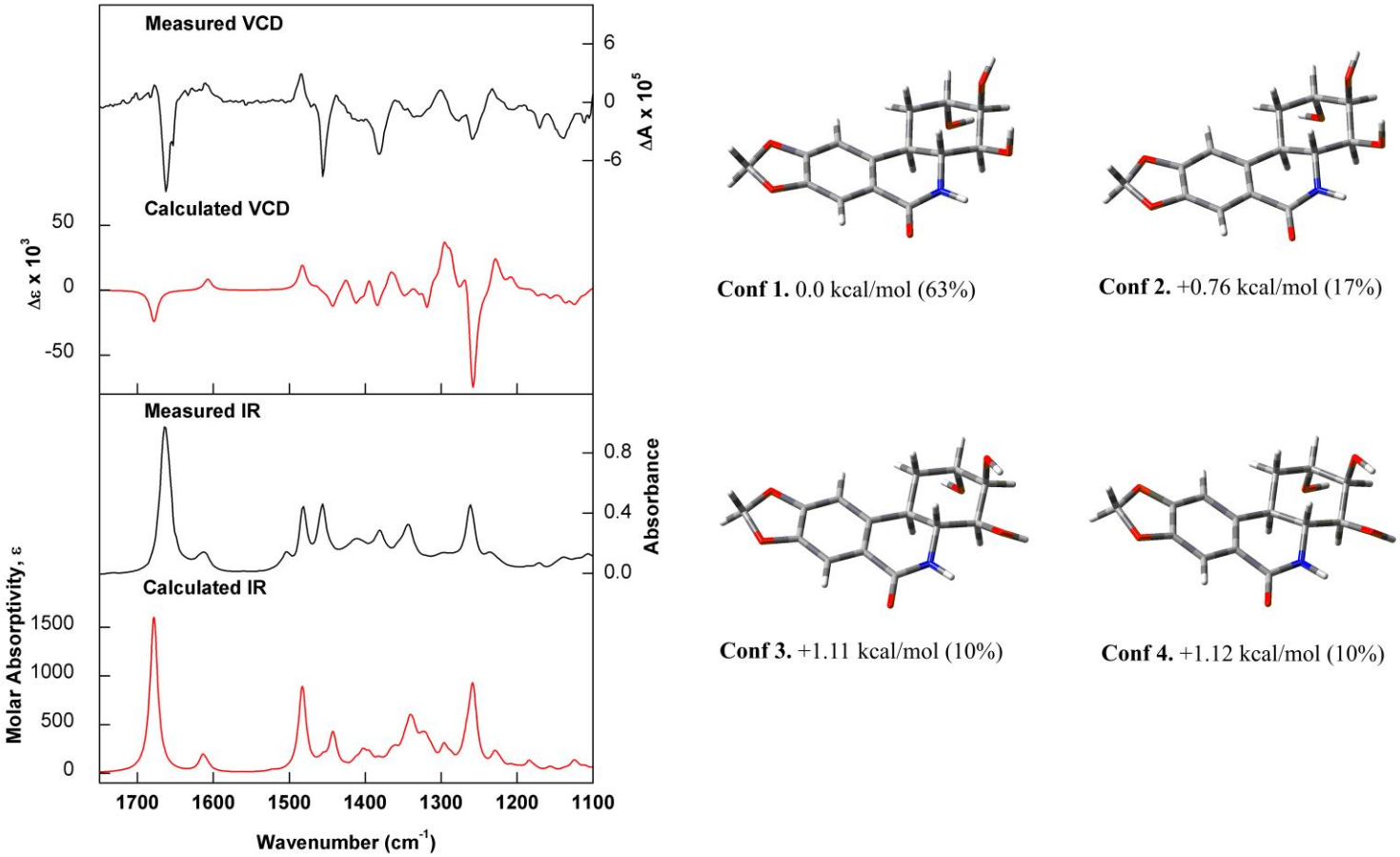

Figure S21. (Left) Comparison of the observed IR and VCD spectra of compound **2** in DMSO-d_6 with the calculated [B3LYP/PCM(DMSO)/6-31G(d)] IR and VCD spectra of the Boltzmann average of the lowest-energy conformers identified for (2*S*,3*R*,4*S*,4a*R*10b*R*)-**2**. (Right) Optimized structures, relative Gibbs free energies, and Boltzmann population (%) of the lowest-energy conformers of (2*S*,3*R*,4*S*,4a*R*10b*R*)-**2**at the B3LYP/PCM(DMSO)/6-31G(d) level.

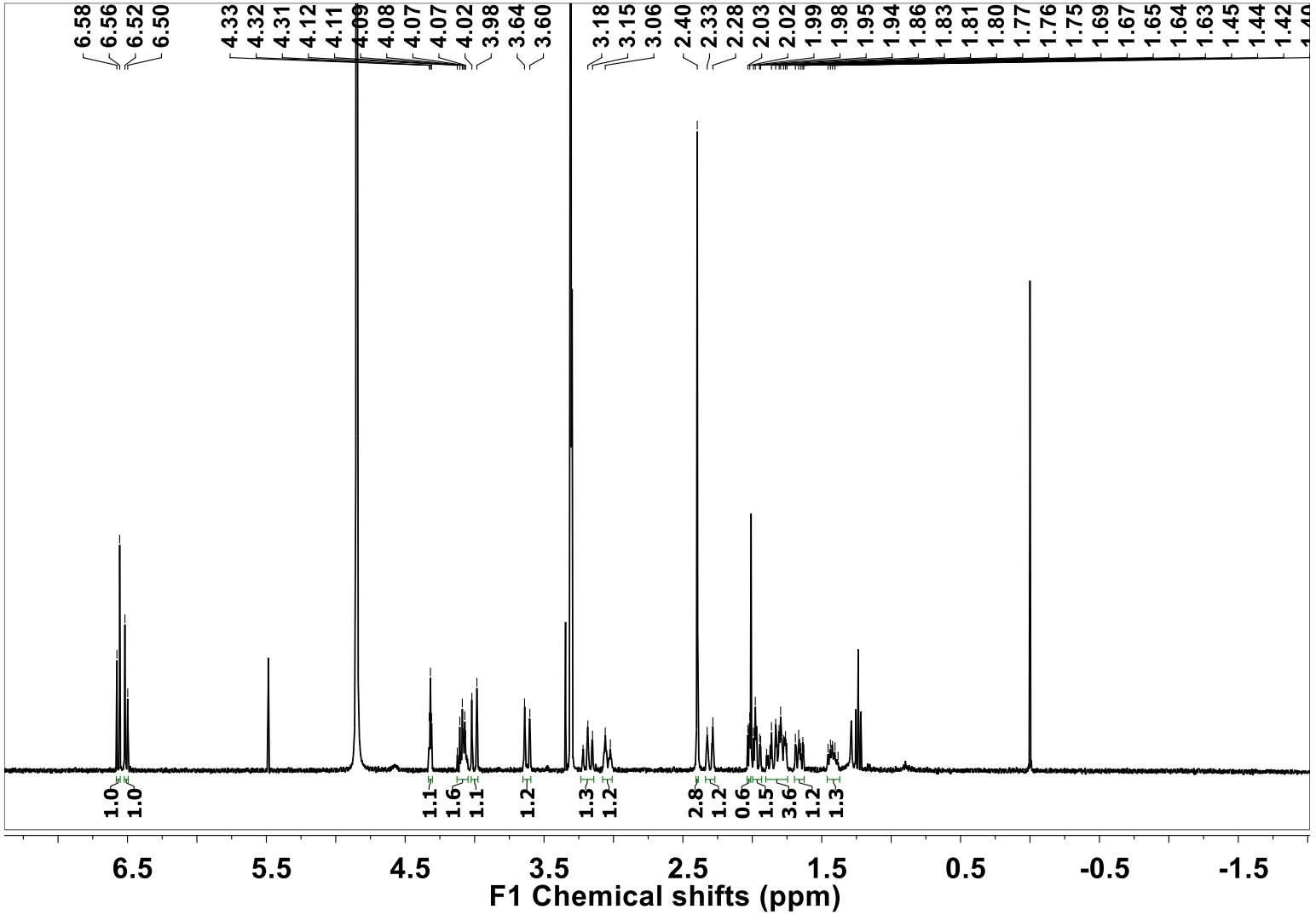

Figure S22. ^{1}H NMR spectrum of compound **6** (400 MHz, MeOD).

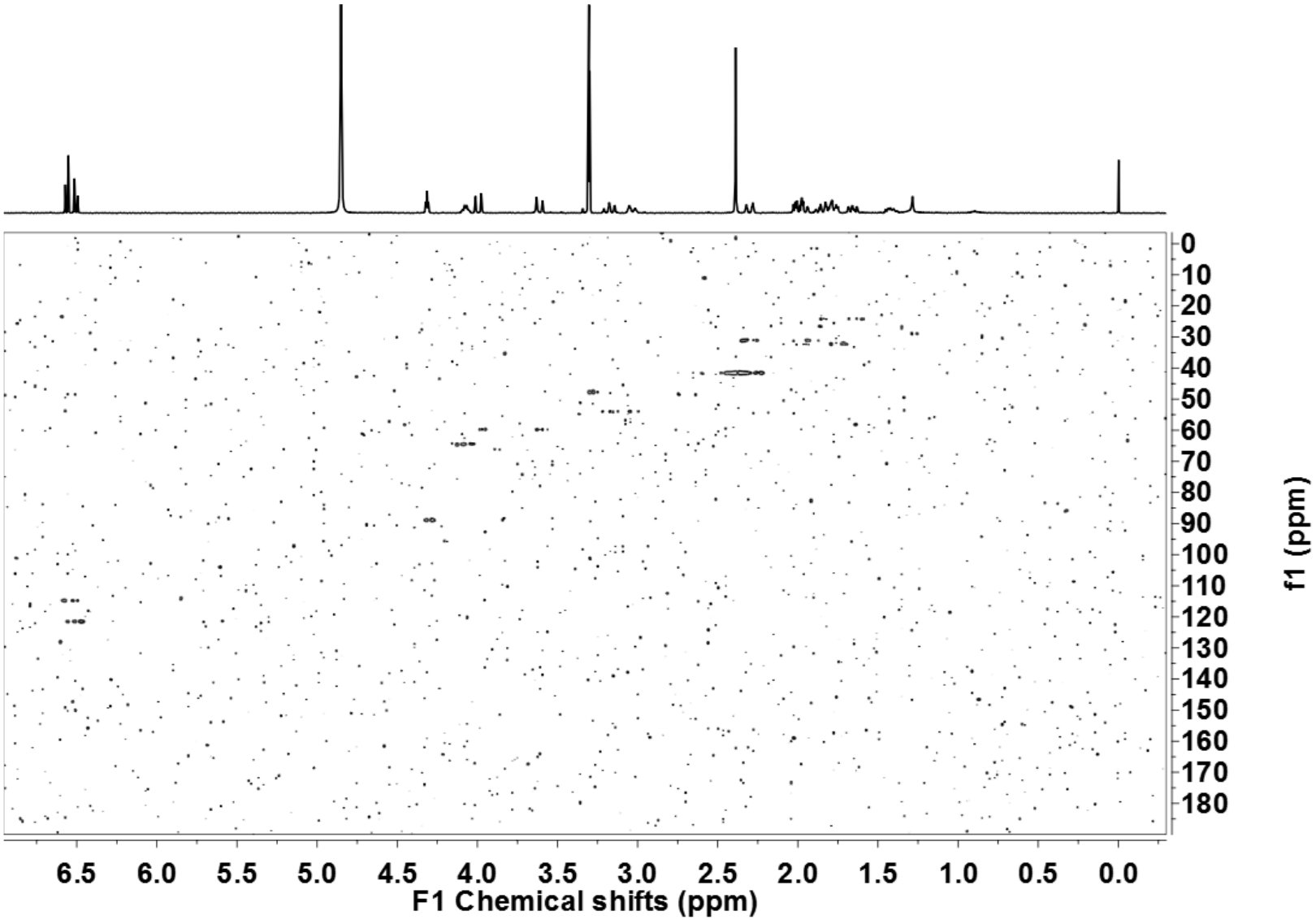

Figure S23. HSQC spectrum of compound **6** (400 MHz, MeOD).

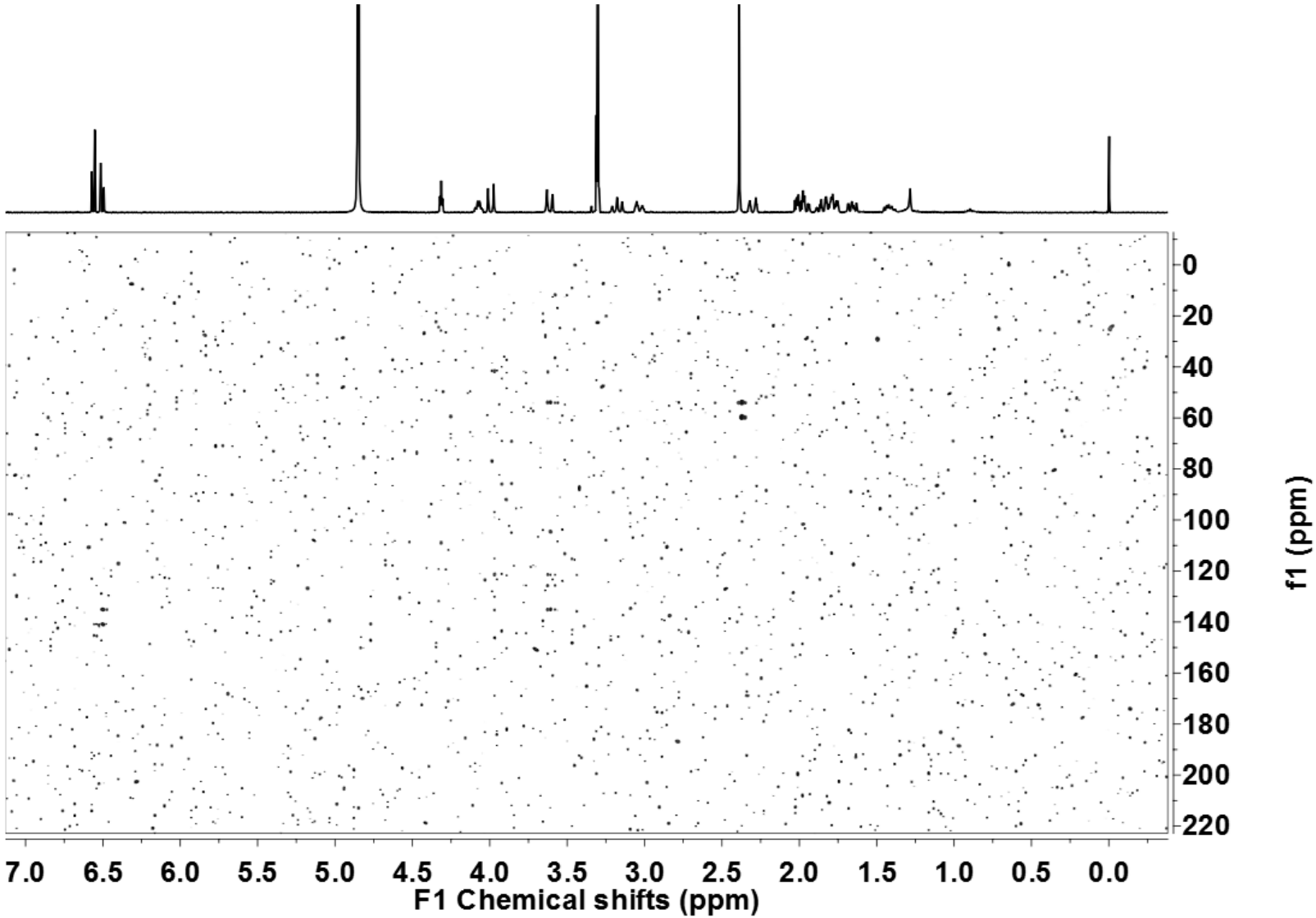

Figure S24. HMBC spectrum of compound **6** (400 MHz, $CDCl_3$).

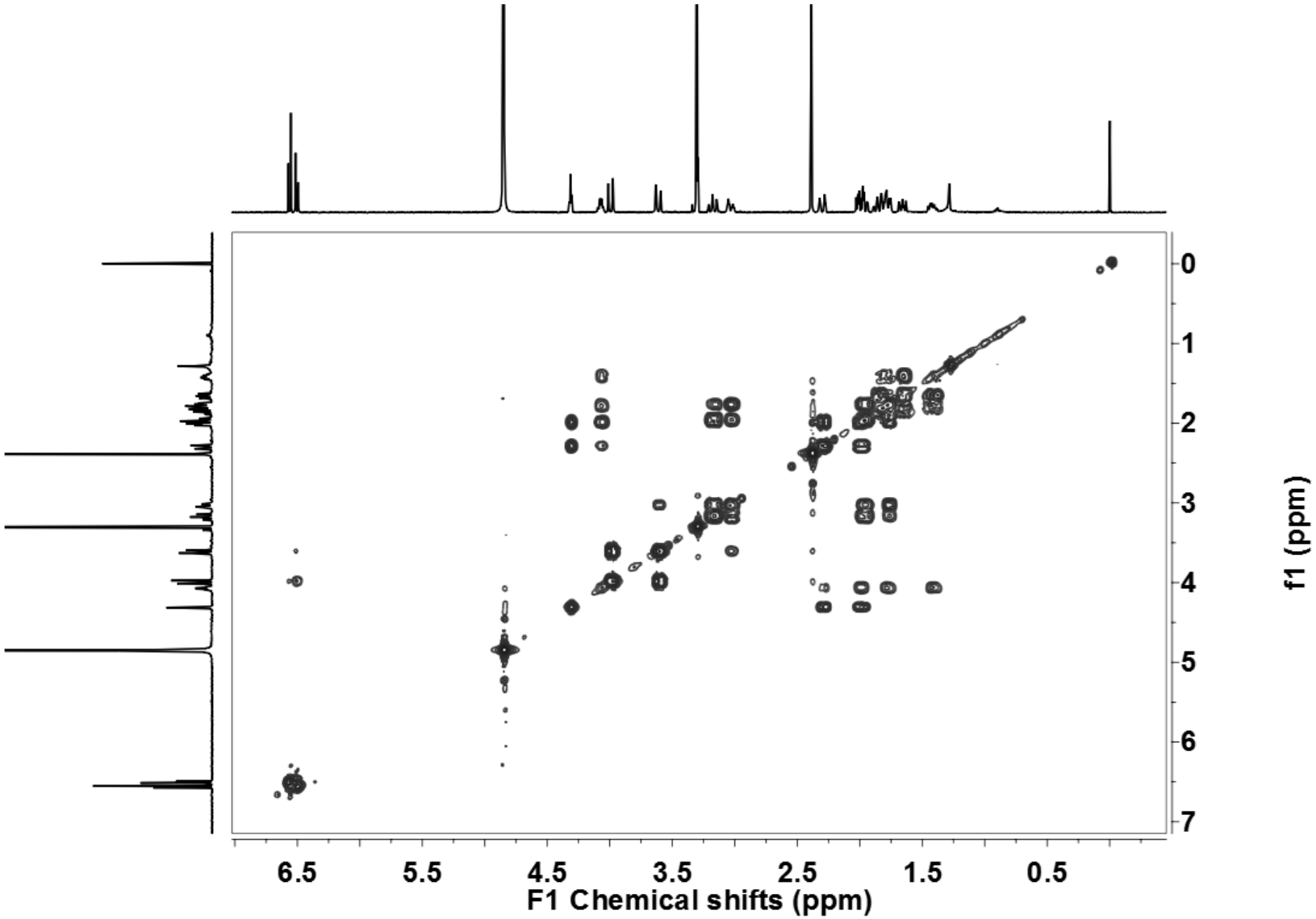

Figure S25. COSY spectrum of compound **6** (400 MHz, $CDCl_3$).

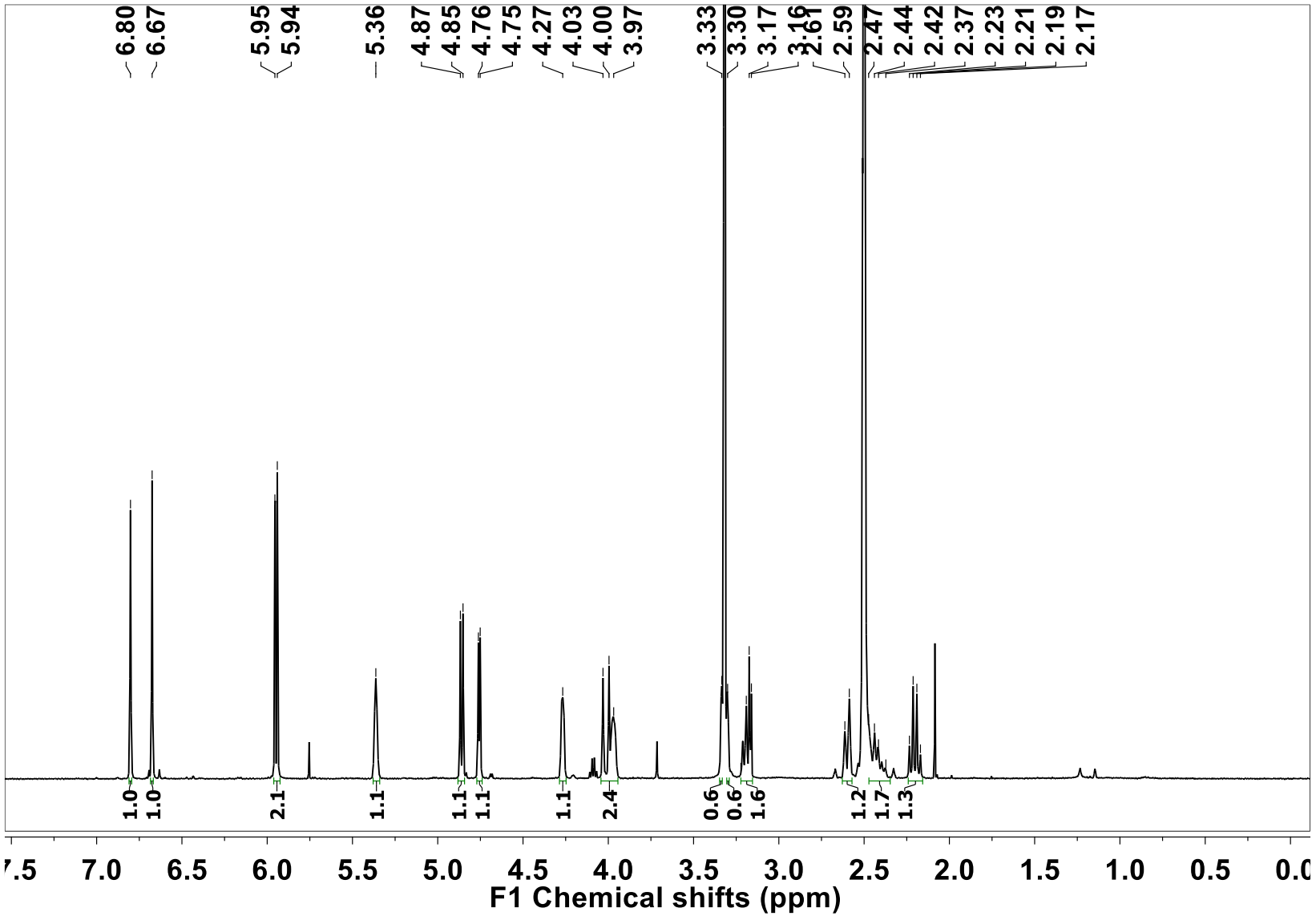

Figure S26. ^{1}H NMR spectrum of compound **11** (400 MHz, DMSO-d_6).

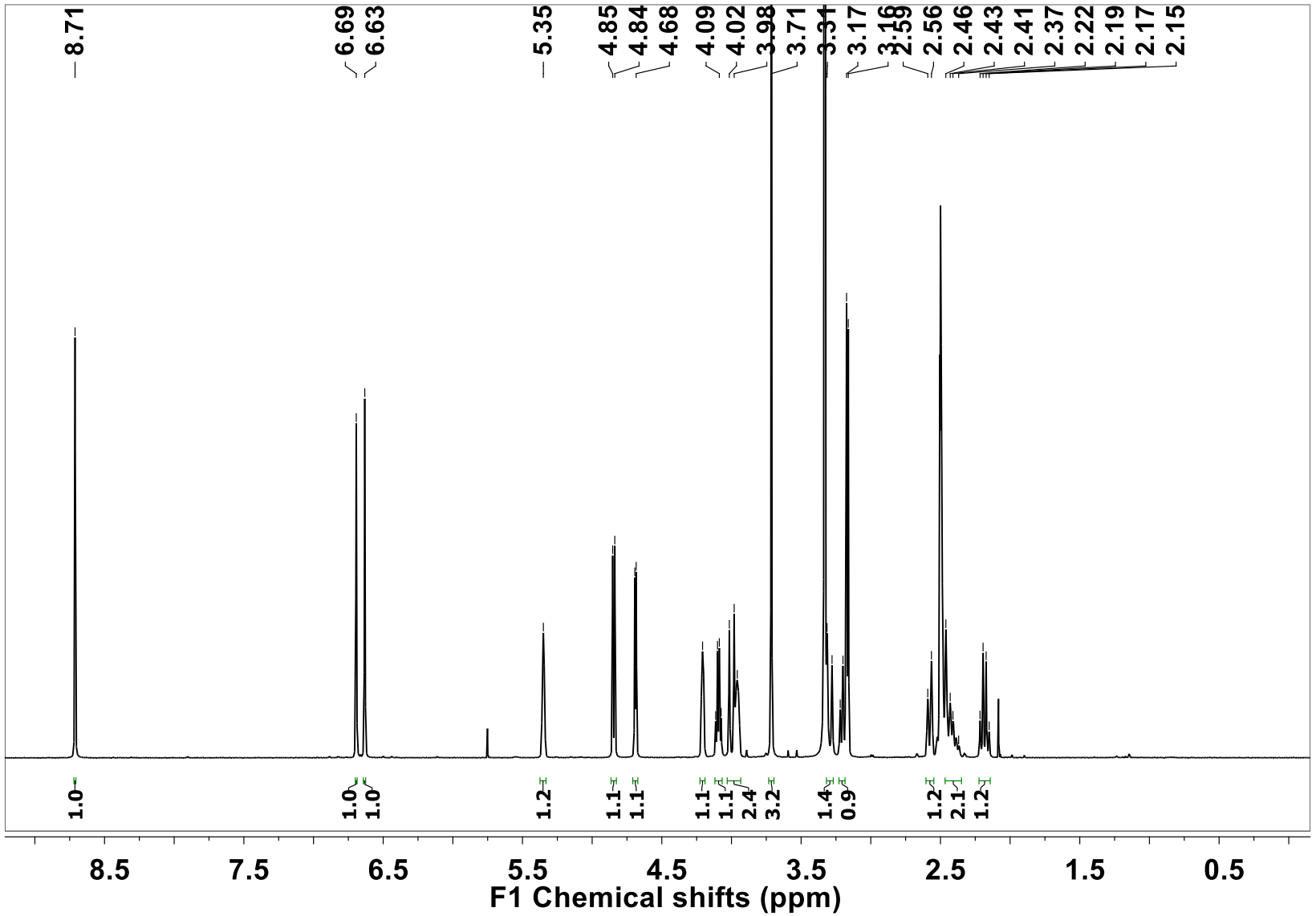

Figure S27.[1]H NMR spectrum of compound **13** (400 MHz, DMSO-d_6).

Table S1. ^{1}H NMR data of compounds **11** and **13** (400 MHz, DMSO-d_6) with comparison to the literature (300 MHz, DMSO-d_6)[1]

Position	Compound **11**	Compound **11**	Compound **13**
	δ_H, mult. (J / Hz)	δ_H, mult. (J / Hz)[1]	δ_H, mult. (J / Hz)
1	4.27 d (4.0)	4.27 br s	4.21 br s
2	3.97 m	3.97 br s	3.96 br s
3	5.36 s	5.37 br s	5.35 br s
4	–	–	–
4a	2.60 d (10.6)	2.60 d (10.6)	2.57 br d (10.1)
6	3.32 d (14.0)	3.32 d (14.4)	3.30 d (14.1)
6'	4.02 d (14.0)	4.02 d (14.4)	4.00 d (13.7)
6a	–	–	–
7	6.67 s	6.68 s	6.63 s
8	–	–	–
9	–	–	–
10	6.80 s	6.81 s	6.69 s
10a	–	–	–
10b	2.50 m	2.50 m	2.47 m
11	2.40 m	2.44 m	2.42 m
12	2.20 dd (8.9:8.4)	2.19 ddd (14.4:8.6:1.5)	2.16 dd (8.8:8.6)
12'	3.19 dd (9.0:8.0)	3.19 dd (14.4:7.5)	3.20 dd (8.4:7.1)
1-OH	4.87 d (6.1)	4.79 br d (2.9)	4.85 d (6.2)
2-OH	4.76 d (4.5)	4.99 br s	4.69 d (4.0)
OCH_2O	5.94 s and 5.95 s	5.94 s and 5.96 s	–
8-OCH_3	–	–	3.71 s
9-OH	–	–	8.71 s

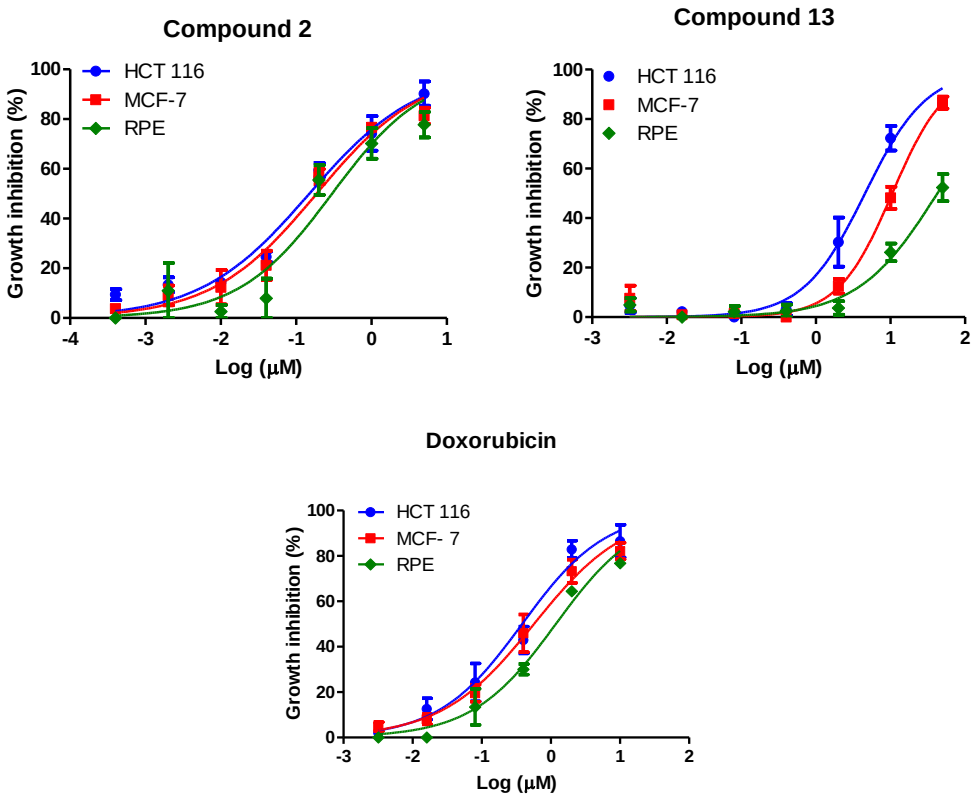

Figure S28. Cytotoxicity of compounds **2** and **13** (0.0032-50 µM) and the positive control doxorubicin (0.0032-10 µM) treatments after 72 h in colorectal carcinoma (HCT 116), breast carcinoma (MCF-7), and non-tumor human retinal epithelial pigment (RPE) cell lines. Data showed as mean and standard error of the mean (mean ± SEM) from three independent experiments performed in duplicate, analyzed by nonlinear regression.

Reference

1. Likhitwitayawuid, K.; Angerhofer, C. K.; Chai, H.; Pezzuto, J. M.; Cordell, G. A.; Ruangrungsi, N.; *J. Nat.Prod.* **1993**, *56*, 1331.